# Radial Electric Field Measurements in Reversed Shear Plasmas

F. M. Levinton,[1] R. E. Bell,[2] S. H. Batha,[3] E. J. Synakowski,[2] and M. C. Zarnstorff[2]

[1]*Fusion Physics and Technology, Torrance, California 90503*
[2]*Princeton Plasma Physics Laboratory, Princeton, New Jersey 08543*
[3]*Science Research Laboratory, Somerville, Massachusetts 02143*

Measurements of the radial electric field have been obtained on the Tokamak Fusion Test Reactor utilizing the motional Stark effect diagnostic. A large negative excursion in the radial electric field occurs before the transition to the enhanced reversed magnetic shear mode. The electric field is localized to a narrow spatial region and is not observed in discharges without the transition to improved confinement. Concomitant with the radial electric field excursion is a change in the measured impurity poloidal rotation velocity and bursts of magnetic fluctuations. [S0031-9007(98)06252-8]

The radial electric field and/or its derivative has recently emerged as a key element in reducing particle and thermal transport in plasmas in a number of different circumstances [1–3]. One paradigm that has been suggested [4] in which $E \times B$ induced velocity shear reduces the growth and radial extent of turbulent eddies in the plasma thereby resulting in lower cross-field transport. This model, which appears generally consistent with transport improvements at the plasma edge in $H$ modes [5], has also been successfully applied to transport reduction in the plasma core of the $VH$ mode [6,7], supershot [8], enhanced reversed shear (ERS) [9–12], and negative central shear (NCS) [13,14] confinement regimes. Other models have been proposed that involve the radial electric field causing a change in the trapped particle orbits which can lead to elimination of banana orbits and trapped particle instabilities along with a reduction in neoclassical transport [15,16].

The critical quantity to measure for further understanding of the physical processes involved is the radial electric field ($E_r$) profile. To date, direct electric field measurements have been made at the plasma edge using Langmuir probes. The radial electric field has also been inferred by measuring the plasma flow velocity and pressure distribution and applying the force balance equation to compute $E_r$. In a toroidally confined plasma, the radial electric field enters the force balance for each plasma species perpendicular to the flux surfaces. From the ion pressure balance, it is given by

$$E_r = (Z_i e n_i)^{-1} \nabla_r p_i + v_{\phi i} B_\theta - v_{\theta i} B_\phi, \quad (1)$$

where $Z_i$ is the charge of the ion, $p_i$ is the ion pressure, $n_i$ is the ion number density, $e$ is the electronic charge, $v_{\phi i}$, $v_{\theta i}$ are, respectively, the ion toroidal and poloidal flow velocities, and $B_\phi$, $B_\theta$ are, respectively, the toroidal and poloidal magnetic fields. This equation applies separately to each ion species and is valid at each point on a flux surface. There are data, both direct and inferred, on the electric field at the plasma edge relating to the physics of the $H$ mode. However, the poloidal rotation velocity profile has been difficult to measure due to poor spatial

resolution [17]. Thus, there is a strong need for a direct $E_r$ measurement. Previous techniques to measure $E_r$ in the central region of a hot plasma have used a heavy-ion beam [18]. Very high energies are required, even for moderate size devices, so this technique has not been applied on experimental devices that are large or have high magnetic fields.

A new approach has been developed to measure $E_r$ [19,20] based on the motional Stark effect (MSE) [21,22]. The MSE diagnostic was developed to measure the safety factor ($q$ profile) which plays a fundamental role in determining the equilibrium and stability of plasmas in toroidal magnetic confinement configurations. It has become the preferred technique for this measurement due to its excellent spatial and temporal resolution combined with its high accuracy and nonperturbing implementation. As a neutral beam of hydrogenic atoms propagates across a magnetic field, an electric field, $E_m = V_b \times B$, will be induced in the atom's frame, where $V_b$ is the beam velocity and $B$ is the magnetic field. The electric field causes spectral splitting and polarization of the emitted radiation, known as the Stark effect. Assuming that there are no other electric fields present, then the direction of the polarized emission is a measure of the local direction of the magnetic field. This is directly related to the safety factor by numerical solution of the Grad-Shafranov equation [23].

In a plasma with a substantial pressure gradient or rotation, the radial electric field can be significant and can affect the interpretation of the MSE measurement. With the plasma radial electric field included, the measured polarization angle from MSE is modified,

$$\tan(\gamma_m) = \frac{v_b B_\theta \cos(\alpha + \Omega) + E_r \cos(\Omega)}{v_b B_\phi \sin(\alpha)}, \quad (2)$$

where $\gamma_m$ is the measured pitch angle, $v_b$ is the beam velocity, $\alpha$ is the angle between the neutral beam and the toroidal field, and $\Omega$ is the angle between the measurement sight line and the toroidal field, as shown in Fig. 1. In order for the MSE diagnostic to determine both the magnetic field pitch angle and the radial electric field,
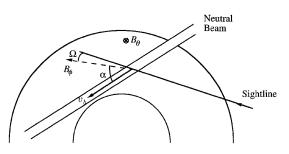
FIG. 1.   Viewing geometry for the MSE diagnostic and neutral beam on TFTR.  Twenty sight lines cover from inboard of the magnetic axis to the outboard plasma edge.

$E_r$, two independent measurements are required.  One approach is to use different viewing angles, which have a different sensitivity to $E_r$.  Then the difference between the two measurements will allow a separation of the magnetic field and the electric field.  Alternatively, using different velocity components from the neutral beam will also permit unfolding of the electric and magnetic fields. Each approach will have different characteristics of spatial resolution and sensitivity [19].  On the Tokamak Fusion Test Reactor (TFTR) we chose to add detectors to measure the pitch angle of the neutral beam half-energy component. This, combined with the full energy component previously used for the MSE measurement provides a measure of $E_r$. This approach has the advantage of using the same sight lines and collection optics and has good spatial resolution. The disadvantage is that the uncertainty of the radial electric field is larger compared with other techniques, due to the increased beam attenuation of the half-energy component and a smaller measured pitch angle difference between the full and half-energy measurements for a given $E_r$.  The instrument on TFTR had half-energy detectors for four channels covering a portion of the major radius from 3.08 to 3.20 m.  This covers the region where the plasma radial electric field was expected to be largest and does not suffer from too much beam attenuation.  Shown in Fig. 2(a) is the time evolution of the measured MSE pitch angle at $R = 3.08$ m ($r/a = 0.35$) for both the full and half-energy signals.  The resulting $E_r$ is shown in Fig. 2(b).  In most cases the electric field was quite small; however, in this example, the change in $E_r$ was so large, localized, and short in duration that it is readily separable from the magnetic field contribution, which can only vary on a much longer time scale, characteristic of the magnetic diffusion through the highly conductive plasma.  One way to separate the $E_r$ from the magnetic field contribution is to use the equilibrium reconstruction to fit the pitch angle profile without the single sight line that exhibits the large transient $E_r$ change.  Then the difference between the fitted and measured pitch angles is the $E_r$ contribution.  The MSE pitch angle computed by the VMEC equilibrium code [23] without using the affected sight line is also shown in Fig. 2(a) for this discharge.  The electric field from the resulting difference is shown in Fig. 2(b), which is in good agreement compared to the $E_r$ measured by the half-energy channel.  The time resolution for this data is 10 ms
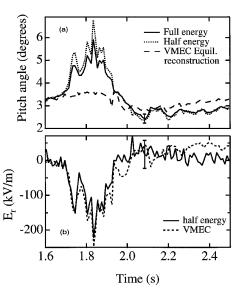
FIG. 2.   (a) Time evolution of the MSE pitch angle at $R = 3.08$ m ($r/a = 0.35$) for the full (solid line) and half-energy (dotted line) signals and the VMEC (dashed line) reconstruction. (b) The corresponding $E_r$ deduced from the full/half-energy difference (solid line) and the full energy/VMEC difference (dashed line).

and has a statistical uncertainty of 17 kV/m, while the systematic uncertainty is estimated to be about 40 kV/m. The systematic uncertainty results mainly in an overall offset to the data while the statistical uncertainty manifests itself as random noise.  The statistical uncertainty can be reduced to about 10 kV/m with some loss of time resolution.

Above some neutral beam power threshold TFTR reversed magnetic shear plasmas [24] exhibit a strong reduction in transport, known as the ERS mode [9].  The transition into the ERS mode is characterized by a rapid rate of rise of the core density caused by a precipitous drop in the particle, ion thermal and momentum transport. At the same time there is a substantial decrease in the density fluctuation level [25].  Reversed shear plasmas were formed by neutral beam injection early in the current ramp phase.  This produced a hollow current profile with a minimum in the $q$ profile, $q_{min}$, at $r/a \sim 0.3 - 0.5$.  This was followed by a high power neutral beam injection phase with input powers ranging from 12–30 MW. The discharges that have been studied with the new $E_r$ measurements had toroidal fields of 4.6 and 3.4 T and with plasma currents of 1.6 and 1.2 MA, respectively.  In discharges that made an ERS transition, a transient and localized radial electric field often appeared 20–60 ms after the high power heating phase began and 60–100 ms prior to the transition.  This phenomenon was previously observed in measurements of the carbon poloidal rotation velocity [26].  In discharges without ERS transitions we have not observed large $E_r$ excursions.  The change in $E_r$ can be over $-250$ kV/m, compared to an $E_r$ level of 10–20 kV/m before the excursion, and was usually observed on only one of the MSE sight lines, which have a

separation of 4 cm. Shown in Fig. 3 is the time evolution of the pitch angle at three radii. The $R = 3.04$ m sight line shows the effect on the pitch angle of the $E_r$ excursion between 1.75 and 2.0 s. The two adjacent sight lines show little or no indication of any electric field. If the width of the $E_r$ excursion was less than the sight line width or spatial resolution of 3.5 cm, then the instrument would underestimate the real $E_r$ change due to the spatial averaging of the measurement. The neutral beam power was increased from 8 to 12.5 MW at 1.7 s. At 1.85–1.90 s the transition into ERS occurs. The large $E_r$ excursion consistently happens before the ERS transition, but the magnitude of $E_r$ can vary significantly from shot to shot. The location of the change in $E_r$ is just inboard of $r_{min}$, the location of the minimum of the $q$ profile. This is also approximately where the ERS transport improvement begins. The $E_r$ excursions appear to happen just before $q_{min}$ reaches an integer value of $q_{min} = 2$ or 3. In our limited set of data, the largest $E_r$ excursion occurs at the lower toroidal field when $q_{min} = 2.2 \pm 0.18$. In discharges with $q_{min} \sim 3.2$, at 4.6 or 3.4 T, the $E_r$ change is smaller.

Measurements of the chord averaged carbon poloidal rotation on TFTR also shows a large excursion [26] concomitant with the radial electric field transient measured by MSE. The time evolution and the temporal structure of the $E_r$ excursion from the MSE data and the poloidal velocity excursion look remarkably similar, as shown in Fig. 4. This is consistent with radial force balance, Eq. (1), since the pressure and toroidal velocity show little change during this time. The MSE $E_r$ measurement shown has a temporal averaging time of 5 ms resolution, and for the poloidal velocity it is 20 ms. The statistical uncertainty of the chordal poloidal velocity measurement is 0.1 km/s. Quantitatively one can compare the change in $E_r$, during the excursion, between MSE and the poloidal velocity at the time of peak change, which is at 1.81 s, as shown in Fig. 4. The change is a better comparison since the absolute values can differ due to systematic uncertainties as well as contributions from the pressure gradient and toroidal velocity terms in Eq. (1). The apparent change in
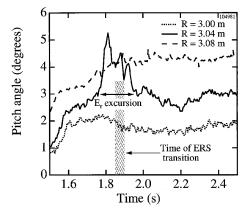
chord averaged poloidal velocity corresponds to a change in $E_r$ of about $-120$ kV/m, using Eq. (1) and a toroidal field of 3.0 T at the location of the sight line shown in Fig. 4. This is within a factor of 2 of the corresponding change in $E_r$ from MSE, which is about $-200$ kV/m. We can reasonably expect the inversion of the poloidal velocity [17] to increase, giving better agreement with the MSE data. Also, the viewing sight lines of the two diagnostics are a few centimeters apart, and with the very narrow localization of $E_r$ of less than 3.5 cm it may be different at the two locations.

Several physical models have been hypothesized to explain the reduced transport in various regimes. A theory that has emerged as a leading candidate is $\mathbf{E} \times \mathbf{B}$ induced velocity shear that reduces the growth and radial extent of turbulent eddies in the plasma resulting in reduced cross-field transport. Studies of the ERS transition mechanism in TFTR have been done for both the start of the transition, which occurs shortly after the beginning of the high power phase, as well as the back transition, in a lower power "postlude" phase when the plasma undergoes a transition out of the ERS mode. For the postlude studies [10] it was found that the plasma remained in the ERS mode when a characteristic shearing rate [27,28],

$$\omega_{E \times B} = \frac{(RB_\theta)^2}{B} \left( \frac{\partial}{\partial \psi} \right) \frac{E_r}{RB_\theta} , \qquad (3)$$

exceeded the linear growth rate of the fastest growing mode, as calculated from a linear gyrofluid model [29]. Typical values of the growth rate and flow shear rate are $<2 \times 10^5$ s$^{-1}$ [10,11]. However, for comparisons at the start of the ERS transition, the agreement was not as good. At the lower magnetic field the flow shear rate was about a factor of 3 below the growth rate, whereas at the higher magnetic field they were equal [11]. These comparisons were based on a neoclassical calculation of the poloidal velocity, without benefit of $E_r$ or poloidal velocity measurements. In light of these new measurements of $E_r$ the flow shear rate, during the excursion, is more than an order of magnitude larger than was previously estimated and would significantly exceed



FIG. 3. The magnetic field pitch angle evolution of three sight lines. The time of the ERS transition is at 1.85–1.90 s.
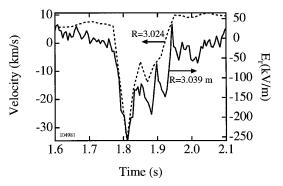


FIG. 4. The time evolution of $E_r$ (solid line) from MSE and the measured poloidal rotation velocity (dashed line) at similar radii.
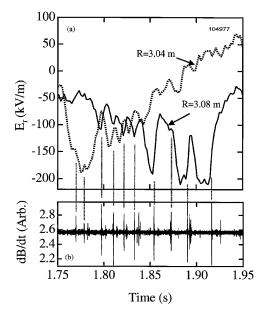
FIG. 5. (a) The time evolution of $E_r$ at two radii and (b) Mirnov coil signal with MHD bursts correlated with changing $E_r$.

the linear growth rates required to stabilize the turbulence and trigger an ERS transition.

With large changes in the radial electric field and poloidal rotation it is natural to expect other effects on the plasma. During the time interval of the large $E_r$ and $V_\theta$ excursions there are occasional coherent magnetic field fluctuations observed on Mirnov pickup coils with frequency components near 50 and 250 kHz. The 50 kHz mode usually precedes the 250 kHz burst. The lower frequency mode has a toroidal mode number of $n = 1$, while the higher frequency mode has a best fit for $n = 0$. The bursts last for 0.2–0.3 ms. The mode is also observed on the electron cyclotron emission (ECE) diagnostic and is localized very near the radius of $q_{min}$. This MHD activity has no effect on the plasma stored energy or other parameters. Changes in the magnitude of $E_r$ are correlated with the timing of the MHD bursts. On a discharge where $E_r$ appears on two channels, the burst coincides with an increase of $E_r$ at one channel and a decrease at the other channel, as shown in Fig. 5. The correlation of the changes in $E_r$ between the two sight lines is probably caused by some motion of the $E_r$ location. The instability has not yet been identified; however, with the large gradient in the poloidal flow providing a source of free energy, the Kelvin-Helmholtz [30] instability is a possible candidate. Usually the shear in the magnetic field is sufficient to stabilize this instability [4,31], but with the gradients in $E_r$ occurring near $q_{min}$, where the magnetic shear is very weak, the plasma may be susceptible to this instability.

In conclusion, $E_r$ measurements in TFTR have been demonstrated using the combination of full and half neutral beam energy components. The large and localized changes in $E_r$ and $V_\theta$ appear to trigger a transition to the ERS mode and precipitate an MHD instability. The cause or the drive

mechanism for $E_r$ and the poloidal flow is unknown. With the significant variation in the magnitude of $E_r$ from shot to shot and the limited set of data, it is not known what the parametric dependence is of $E_r$, but with this and further studies of $E_r$ it is likely to provide important insight into our basic understanding of plasma transport.

[1] R. J. Taylor et al., Phys. Rev. Lett. **63**, 2365 (1989).
[2] R. J. Groebner, K. H. Burrell, and R. P. Seraydarian, Phys. Rev. Lett. **64**, 3015 (1990).
[3] R. R. Weynants et al., Nucl. Fusion **32**, 837 (1992).
[4] H. Biglari, P. H. Diamond, and P. W. Terry, Phys. Fluids B **2**, 1 (1990).
[5] F. Wagner et al., Phys. Rev. Lett. **49**, 1408 (1982).
[6] G. L. Jackson et al., Phys. Rev. Lett. **67**, 3098 (1991).
[7] K. H. Burrell et al., Phys. Plasmas **1**, 1536 (1994).
[8] D. R. Ernst et al., Phys. Plasmas **5**, 665 (1998).
[9] F. M. Levinton et al., Phys. Rev. Lett. **75**, 4417 (1995).
[10] E. J. Synakowski et al., Phys. Rev. Lett. **78**, 2972 (1997).
[11] F. M. Levinton et al., in *Fusion Energy 1996, Montreal, Canada* (International Atomic Energy Agency, Vienna, 1997), Vol. 1, p. 211.
[12] E. J. Synakowski et al., Phys. Plasmas **4**, 1736 (1997).
[13] E. J. Strait et al., Phys. Rev. Lett. **75**, 4421 (1995).
[14] K. H. Burrell, Phys. Plasmas **4**, 1499 (1997).
[15] A. B. Hassam, Nucl. Fusion **36**, 707 (1996).
[16] J. Nycander and V. V. Yankov, JETP Lett. **63**, 448 (1996).
[17] R. E. Bell, Rev. Sci. Instrum. **68**, 1273 (1997).
[18] F. C. Jobes and R. L. Hickok, Nucl. Fusion **10**, 195 (1970).
[19] M. C. Zarnstorff, F. M. Levinton, S. H. Batha, and E. J. Synakowski, Phys. Plasmas **4**, 1097 (1997).
[20] B. W. Rice, K. H. Burrell, L. L. Lao, and Y. R. Lin-Liu, Phys. Rev. Lett. **79**, 2694 (1997).
[21] F. M. Levinton et al., Phys. Rev. Lett. **63**, 2060 (1989).
[22] F. M. Levinton, Rev. Sci. Instrum. **63**, 5157 (1992).
[23] S. P. Hirshman et al., Phys. Plasmas **1**, 2277 (1994).
[24] S. H. Batha, F. M. Levinton, M. C. Zarnstorff, and G. L. Schmidt, in *Proceedings of the Twenty-Second European Conference on Controlled Fusion and Plasma Physics, Bournemouth, England, 1995* (European Physical Society, Geneva, 1995), Vol. 2, p. 113.
[25] E. Mazzucato et al., Phys. Rev. Lett. **77**, 3145 (1996).
[26] R. E. Bell, F. M. Levinton, S. H. Batha, E. J. Synakowski, and M. C. Zarnstorff (to be published).
[27] T. S. Hahm and K. H. Burrell, Phys. Plasmas **2**, 1648 (1995).
[28] R. E. Waltz, G. D. Kerbel, and J. Milovich, Phys. Plasmas **1**, 2229 (1994).
[29] M. A. Beer, G. W. Hammett, G. Rewoldt, E. J. Synakowski, and M. C. Zarnstorff, Phys. Plasmas **4**, 1792 (1997).
[30] S. Chandrasekhar, *Hydrodynamic and Hydromagnetic Stability* (Dover, New York, NY, 1981).
[31] B. D. Scott, P. W. Terry, and P. H. Diamond, Phys. Fluids **31**, 1481 (1988).